Carbohydrate Polymers 80 (2010) 533–538

Contents lists available at ScienceDirect

Carbohydrate Polymers

journal homepage: www.elsevier.com/locate/carbpol

Formation of elongated starch granules in high-amylose maize

Hongxin Jiang [a], Harry T. Horner [b], Tracey M. Pepper [b], Michael Blanco [c], Mark Campbell [d], Jay-lin Jane [a,*]

[a] Department of Food Science and Human Nutrition, Iowa State University, Ames, IA 50011, USA
[b] Department of Genetics, Development and Cell Biology & Microscopy and NanoImaging Facility, Iowa State University, Ames, IA 50011, USA
[c] USDA-ARS/Plant Introduction Research Unit, Ames, IA 50011, USA
[d] Truman State University, Kirksville, MO 63501, USA

ARTICLE INFO

Article history:
Received 14 November 2009
Received in revised form 10 December 2009
Accepted 11 December 2009
Available online 16 December 2009

Keywords:
High-amylose maize starch
Amylose-extender mutant
Resistant starch
Starch structure
Long-chain double-helical crystallite
Elongated starch granule
Starch granule formation

ABSTRACT

GEMS-0067 maize starch contains up to 32% elongated starch granules, much higher than amylose-extender (*ae*) single-mutant maize starch (~7%) and normal (non-mutant) maize starch (0%). These elongated granules are highly resistant to enzymatic hydrolysis at 95–100 °C, which function as resistant starch. The structure and formation of these elongated starch granules, however, were not known. In this study, light, confocal laser-scanning, scanning electron, and transmission electron microscopy were used to reveal the structure and formation of these elongated starch granules. The transmission electron micrographs showed fusion through amylose interaction between adjacent small granules in the amyloplast at the early stage of granule development. A mechanistic model for the formation of elongated starch granules is proposed.

© 2009 Elsevier Ltd. All rights reserved.

1. Introduction

Starch exists widely in seeds, roots, tubers, and fruits as an energy reserve of plants (Robyt, 1998). Because starch is a renewable, economical, and environmentally friendly biopolymer, it is widely used in food and non-food applications, such as a thickener, binder, film, and foam (Richardson, Jeffcoat, & Shi, 2000). There has been an increased interest in producing resistant starch (RS) from high-amylose maize starch. RS is a portion of starch that cannot be hydrolyzed by human digestive enzymes and functions as a prebiotic for bacterial fermentation in the large intestine (Englyst & Cummings, 1985; Englyst & Macfarlane, 1986). RS from high-amylose maize starch has been reported to provide many health benefits. When RS is used to replace rapidly digestible starch in food, it lowers the glycemic and insulin responses and reduces the risk for developing type II diabetes, obesity, and cardiovascular disease (Behall, Scholfield, & Hallfrisch, 2006a; Behall, Scholfield, Hallfrisch, & Liljeberg-Elmstaahl, 2006b; Robertson, Bickerton, Dennis, Vidal, & Frayn, 2005; Robertson, Currie, Morgan, Jewell, & Frayn, 2003; Zhang, Wang, Zhang, & Yang, 2007). RS lowers calories of foods (Behall & Howe, 1996) and enhances lipid oxidation (Higgins et al., 2004), which reduce body fat and impact body composition (Pawlak, Kushner, & Ludwig, 2004). Fermentation of RS in the colon promotes a healthy colon and reduces the risk of colon cancer (Dronamraju, Coxhead, Kelly, Burn, & Mathers, 2009; Van Munster, Tangerman, & Nagengast, 1994).

Normal maize starch contains less than 1% RS (AOAC, 2003), whereas starch of maize *ae* single-mutant has ~15% RS (Li, Jiang, Campbell, Blanco, & Jane, 2008). A recently developed GEMS-0067 high-amylose maize starch, through the USDA-ARS Germplasm Enhancement of Maize (GEM) Project, contains up to 43.2% RS (Li et al., 2008). The GEMS-0067 is an inbred line of maize homozygous mutant of *ae* gene and a high-amylose modifier (HAM) gene (Campbell, Jane, Pollak, Blanco, & O'Brien, 2007).

Normal maize starch is composed of ~30% primarily linear amylose and ~70% highly-branched amylopectin, which are organized in granules with a semi-crystalline structure of double helices. Amylose is a polysaccharide of essentially (1→4)-linked α-D-glucopyranose, and exists in an amorphous state within the normal maize starch granule. Amylopectin molecules consist of (α1→6) linked branch-chains of (1→4) α-D-glucopyranose, which contribute to the crystallinity of starch (French, 1984; Jane, Xu, Radosavljevic, & Seib, 1992; Kasemsuwan & Jane, 1994). The GEMS-0067 starch consists of ~85% amylose, much greater than normal maize starch (~30%) and starches of maize *ae* single-mutant (50–70%) (Li, Blanco, & Jane, 2007; Li et al., 2008).

Normal maize starch has starch granules with spherical and angular shapes, whereas high-amylose maize (*ae* single-mutant) starch consists of ~7% elongated granules (Jiang, Campbell, Blanco, & Jane, 2009; Perera, Lu, Sell, & Jane, 2001). The GEMS-0067 starch consists of up to 32% elongated starch granules (Jiang et al., 2010).

* Corresponding author. Tel.: +1 515 294 9892; fax: +1 515 294 8181.
E-mail address: jjane@iastate.edu (J.-l. Jane).

0144-8617/$ - see front matter © 2009 Elsevier Ltd. All rights reserved.
doi:10.1016/j.carbpol.2009.12.016

The elongated starch granules and the outer layer of the spherical starch granules are highly resistant to enzymatic hydrolysis and remain in the RS residue that consists of partially hydrolyzed amylose with molecular weights of DP 411–675 (Jiang et al., 2010). It is of great interest to understand how the elongated starch granules are formed during kernel development and the RS formation in the high-amylose maize starch. In this study, we used different microscopic approaches to reveal the internal structures and the formation of elongated starch granules during kernel development. Combining these results with the chemical structures of the starch crystallites reported previously (Jiang et al., 2010), we propose a mechanism of the development of elongated granules.

2. Materials and methods

2.1. Materials

GEMS-0067 (High-amylose maize) and B73 (normal maize) maize lines were planted in the field at the USDA-ARS North Central Regional Plant Introduction Station (NCRPIS) in Ames, IA in 2007. Plants were self-pollinated by hand pollination, and ears of GEMS-0067 and B73 were harvested on 20 days after pollination (DAP) and after the physiological maturation of the maize kernels (54 DAP).

2.2. Starch isolation

Starch was isolated from mature maize endosperm using the method described by Li et al. (2008).

2.3. Scanning electron microscopy

Images of the starch granules were collected using a scanning electron microscope (JEOL 5800, www.jeol.com) in the Microscopy and NanoImaging Facility, Iowa State University, Ames IA 50011. The starch samples were coated with palladium-gold (60:40) and viewed at 10 kV.

2.4. Light microscopy

Native starch granules were viewed and imaged using polarizing and phase-contrast optics using a compound light microscope (Zeiss Axioplan 2, www.zeiss.com) equipped with a digital AxioCam MRC color camera and Axiovison rel 4.5 software.

2.5. Confocal laser-scanning microscopy (CLSM)

The CLSM was conducted following the method described by Glaring, Koch, and Blennow (2006). Starch (~12% MC, 4.0 mg) was dried at 45 °C using a centrifugal vacuum evaporator for 2 h. Four μL of 8-aminopyrene-1,3,6-trisulfonic acid (APTS, Cat. No. 09341, www.sigmaaldrich.com) solution (0.02 M APTS in 15% acetic acid) and 4 μL of sodium cyanoborohydride (1 M in tetrahydrofuran, Cat. No. 296813, www.sigmaaldrich.com) were added to the dried starch sample. The mixture was incubated at 30 °C for 16 h. The APTS-stained starch granules were viewed using a confocal laser-scanning microscope (TCS SP5 X, www.leica.com) at the Confocal Microscopy and Image Analysis Facility, Iowa State University, Ames IA 50011. A laser beam with 488 nm wavelength was used for excitation. The emission peak was detected between 500 and 535 nm.

2.6. Transmission electron microscopy (TEM)

The endosperm tissues of GEMS-0067 and B73 kernels harvested on 20 DAP were prepared for TEM following the method of Horner et al. (2007). Observations of the fixed tissues were made using a transmission electron microscope (JEOL 2100, www.jeol.com), and images were captured using a high-resolution digital camera (U-1000, www.gatan.com).

3. Results and discussion

3.1. Morphology of GEMS-0067 starch granules

GEMS-0067 starch consisted of mainly spherical and elongated starch granules (Fig. 1) as reported by Jiang et al. (Jiang et al., 2010). The elongated starch granules displayed shapes including rods, filaments, and triangles (Fig. 1). It has been shown that maize *ae*-mutant starches contain elongated granules (Boyer, Daniels, & Shannon, 1976; Mercier, Charbonniere, Gallant, & Guilbot, 1970; Shi & Jeffcoat, 2001; Sidebottom, Kirkland, Strongitharm, & Jeffcoat, 1998; Wolf, Seckinger, & Dimler, 1964) and normal maize starch contains starch granules mainly with spherical and angular shapes (Perera et al., 2001; Wongsagonsup, Varavinit, & BeMiller, 2008). The proportion of the elongated starch granules in the maize *ae*-mutant starches increases with the increase in amylose content (Jiang et al., 2010).

3.2. Birefringence of GEMS-0067 starch granules

The starch granules were viewed both with polarizing (Fig. 2A) and phase-contrast light microscopy (Fig. 2B). Between crossed polarizers, GEMS-0067 starch granules displayed different patterns of birefringence (Fig. 2A). Most spherical starch granules exhibited bright Maltese-crosses (Fig. 2A-a), which were similar to those observed in normal maize starch granules (Wongsagonsup et al., 2008). This birefringence pattern indicated that the starch molecules were aligned in a radial order centered at the hilum (growth center) and were perpendicular to the granule surface. The birefringence patterns of elongated starch granules varied and could be classified into 3 types: type 1 birefringence pattern displayed overlapping of several Maltese-crosses (Fig. 2A-b–d); type 2 birefringence pattern consisted of combinations of one or more Maltese-crosses and weak to no birefringence on other parts of the granule (Fig. 2A-e and f); and type 3 exhibited no birefringence

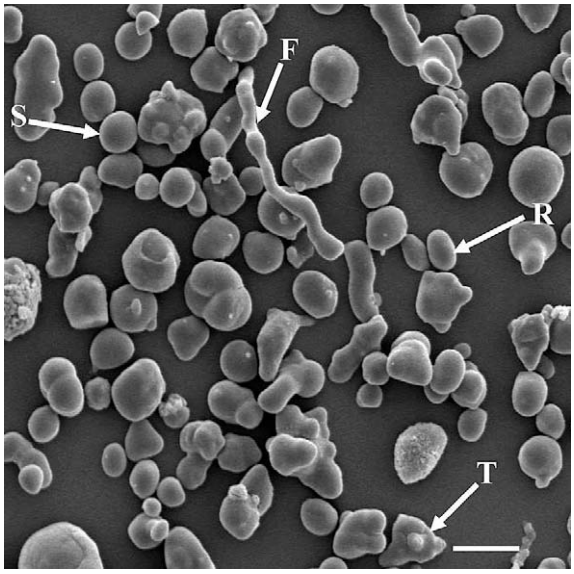

Fig. 1. Scanning electron microscope images of physiologically matured GEMS-0067 starch granules show spherical and elongated granules. Arrows indicate spherical (S), rod (R), filamentous (F), and triangular (T) starch granules. Bar = 10 μm.

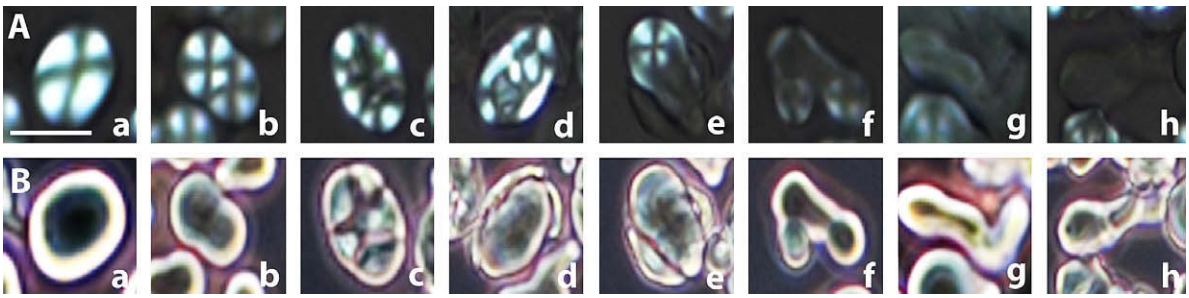

Fig. 2. Polarized (A) and phase-contrast (B) images of GEMS-0067 native starches. (a) spherical granule displaying a single bright Maltese-cross; (b), (c), and (d) type 1 birefringence pattern displaying overlapping of several Maltese-crosses; (e) and (f) type 2 birefringence pattern consisting of one or more Maltese-crosses and weak to no birefringence for remainder of granule; (g) and (h) type 3 birefringence pattern exhibiting weak birefringence along periphery of granule or no birefringence of granule. Bar = 10 μm for all figures.

or only weak birefringence along the edge of the elongated granule (Fig. 2A-g and h). The birefringence patterns of the GEMS-0067 starch granules agreed with that of high-amylose starch reported by Wolf et al. (1964).

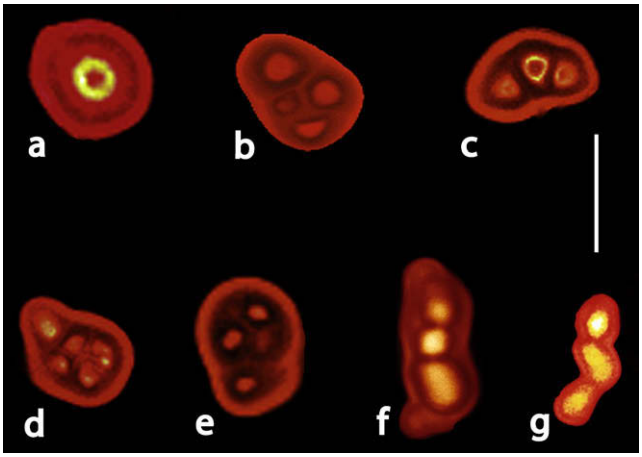

Fig. 3. Confocal laser-scanning microscope images of GEMS-0067 starch granules. (a) spherical granule with bright color in center of granule; (b)–(g) elongated granules with multiple regions differing in intensity of fluorescence. Bar = 10 μm. (For interpretation of the references to colour in this figure legend, the reader is referred to the web version of this article.)

Birefringence patterns are results of orderly aligned polymers or crystallites. Thus, the birefringence patterns of starch granules provide information about the orientations and alignments of starch molecules in different regions of the granule (French, 1984). The different birefringence patterns of the GEMS-0067 starch granules indicated that the arrangement of starch molecules varied between granules and within a granule. The overlapping of several Maltese crosses (Fig. 2A-b–d) in one granule could result from the fusion of starch granules within an amyloplast during the kernel development.

3.3. Internal structure of elongated starch granules

The reductive amination of reducing sugar with a fluorophore, 8-aminopyrene-1,3,6-trisulfonic acid (APTS), has been well studied (Morell, Samuel, & O'Shea, 1998; O'Shea et al., 1998). Because amylose and amylopectin molecules possess reducing ends that could be attached by APTS, CLSM images of APTS-stained starch granules provided information about the internal structure of the starch granules (Glaring et al., 2006). The CLSM images show most spherical granules displaying bright color around one hilum (Fig. 3a), indicating that each of the resulting spherical granules was devel-

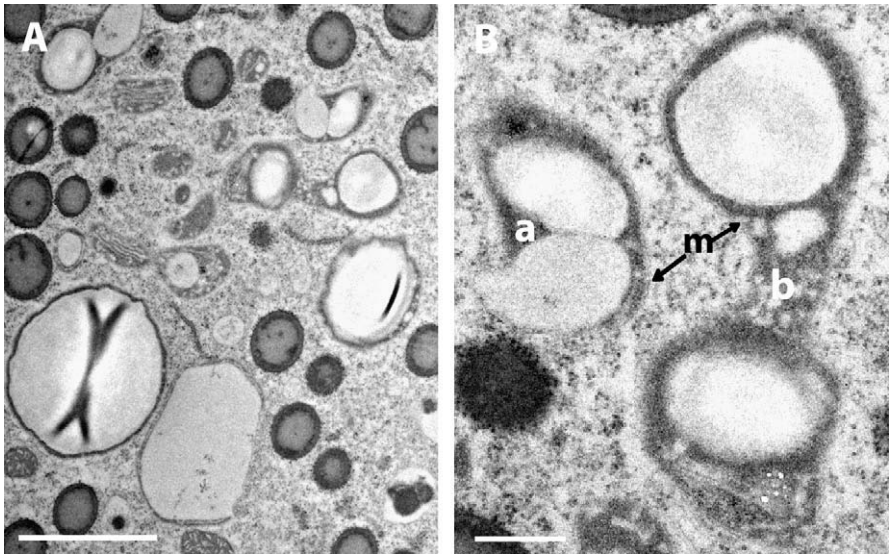

Fig. 4. Transmission electron microscope images of subaleurone layers of B73 (normal maize) endosperm tissue harvested on 20 DAP. (A) overview; (B) higher magnification of A. (a) two starch granules initiated in one amyloplast; (b) amyloplast in division containing two starch granules; m, membrane of amyloplast. Bars = 2 μm on A and 0.5 μm on B.

oped from one single granule. The APTS-staining pattern of the elongated granules revealed multiple regions with different intensities of fluorescence (Figs. 3b–g), similar to that observed by Glaring et al. (Glaring et al., 2006), and indicating that the elongated granules could be formed from the fusion of several small granules.

3.4. Formation of elongated starch granules

To understand starch granule formation during kernel development, endosperm tissues of maize kernels at an early stage were harvested on 20 days after pollination (DAP) and used for TEM studies. TEM images of subaleurone layers from B73 (normal maize) and GEMS-0067 endosperms are shown in Figs. 4 and 5, respectively. Although most mature amyloplasts in B73 endosperm contained only one starch granule as reported by Shannon and Garwood (1984), we observed some amyloplasts contained two starch granules (Fig. 4B–a and b). Fig. 4B-b shows an amyloplast in division containing two starch granules.

Although some amyloplasts at the subaleurone layer of GEMS-0067 endosperm contained only one spherical granule and they displayed normal growth rings and a hilum (Fig. 5A), the majority of amyloplasts contained two or more starch granules (Fig. 5B). Examples of features observed were two starch granules being initiated in one amyloplast, presumably at an early stage of granule development (Fig. 5C); starch granules almost fused (Fig. 5D); and two starch granules fused together forming an elongated starch granule (Fig. 5E). The inner growth rings were each centered around the two hila, but the outer growth rings were integrated into one granule. This elongated starch granule, consisting of two fused granules, agreed with the image of two Maltese-crosses observed in one starch granule (Fig. 2A-b).

Fig. 5F shows two connected starch granules and a third starch granule in the amyloplast protrusion. Three small granules were fused into one granule (Fig. 5G), showing one small granule with a hilum and growth rings, and the other two without hila or growth rings. This elongated starch granule consisted of three

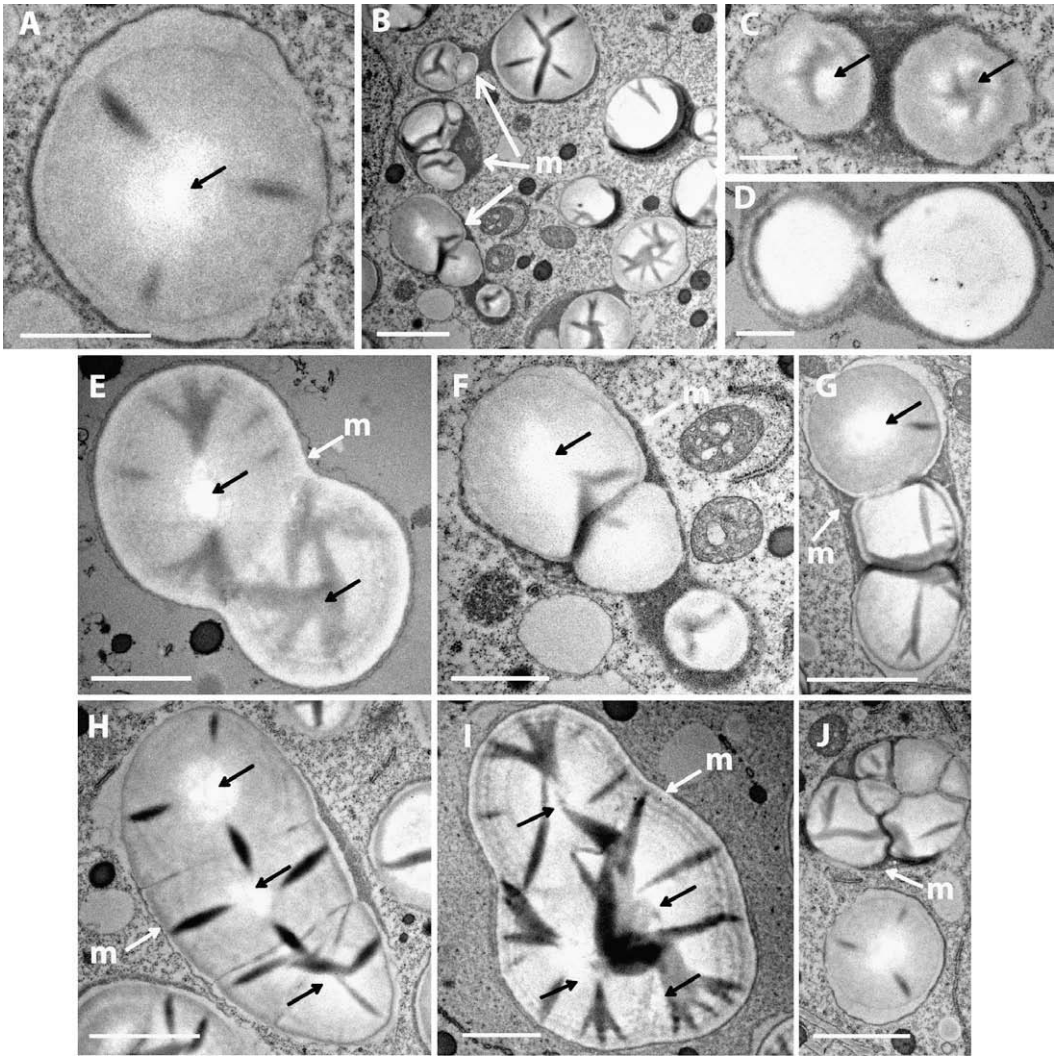

Fig. 5. Transmission electron microscope images of subaleurone layers of GEMS-0067 endosperm tissue harvested on 20 DAP. (A) spherical starch granule with a hilum at center of granule and growth rings; (B) overview of endosperm tissue; (C) two starch granules initiated in one amyloplast at early stage of starch granule development; (D) initial fusion of starch granules; (E) two fused starch granules forming an elongated starch granule; (F) two connected starch granules and a third starch granule in the amyloplast protrusion; (G) three small granules fused into one granule, with one small granule at head showing hilum and growth rings, and the other two granules displaying no hilum or growth rings; (H) elongated starch granule formed by fusion of three small granules, each with a hilum and growth rings; (I) four small starch granules, each with an individual hilum, fused together and coated by several layers of growth rings parallel to boundary of amyloplast; (J) six starch granules, without hila and growth rings, were fused in one amylosplast to form an almost spherical starch granule; m, membrane boundary of amyloplast. Black arrow indicates hilum. Bars = 2 μm on B, E, G, H, I and J; and 1 μm on A, C, D and E.

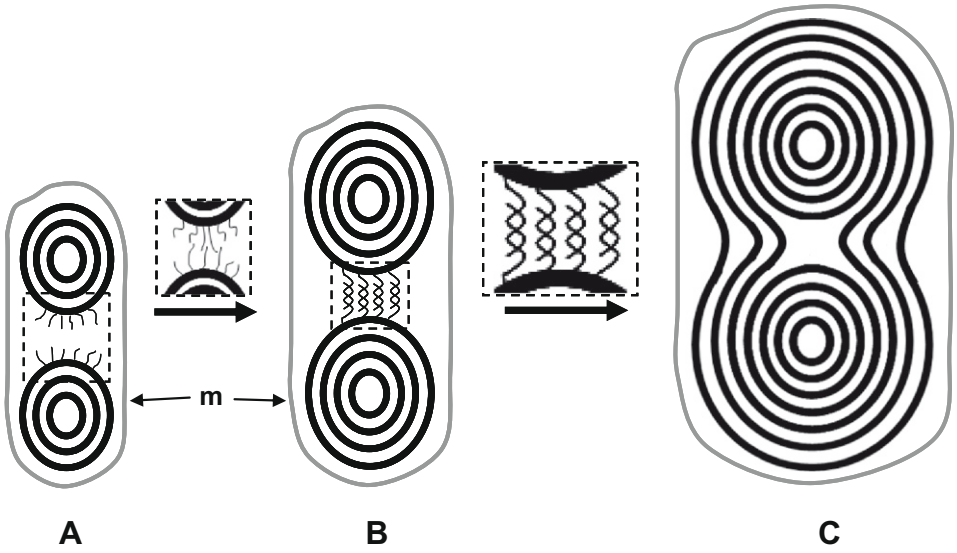

Fig. 6. Proposed model of elongated starch granule formation in amyloplast. (A) two starch granules, each with hilum and growth rings, are initiated in amyloplast; (B) two granules start fusion by amylose interaction forming anti-parallel double helices between them, which prevent amyloplast division; (C) fused granules have integrated outer layer growth rings; m, membrane boundary of amyloplast.

small granules displaying a birefringence pattern with one Maltese-cross at the head and weak to no birefringence in the remainder of the elongated granule (Fig. 2A-e). Fig. 5H shows an elongated starch granule formed from fusion of three small granules, each with a hilum and growth rings. This elongated granule represents the birefringence of the overlapping of Maltese-crosses in the starch granule shown in Fig. 2A-c, and the APTS-stained starch granules shown in Fig. 3c and f.

Fig. 5I shows four small starch granules, each with an individual hilum, fused together and displaying several layers of growth rings parallel to the boundary of the amyloplast. This granule is similar to the APTS-stained starch granules shown in Fig. 3b, d, and e. And in Fig. 5J, six starch granules, without hila and growth rings, were fused in one amylosplast to form an almost spherical starch granule. This granule would have no birefringence when viewed between crossed polarizers.

The TEM images suggest that elongated starch granules are formed from fusion of several small granules, each initiated early in the kernel development. These results support the different birefringence patterns observed using polarizing microscopy and APTS-staining patterns with CLSM for GEMS-0067 starch granules. These fused granules, however, were not observed with B73 normal maize starch.

3.5. Proposed formation mechanism of elongated starch granules

The multiple high-amylose maize starch granules (Fig. 5) appear to fail to separate and retard amyloplast division, resulting in elongated starch granules. Because the GEMS-0067 starch consists of ~85% amylose and the proportion of the elongated starch granules correlates with the amylose content of the starch (Jiang et al., in press), it is plausible that the amylose molecules of an individual granule in the amyloplast interact and form anti-parallel double helices with amylose molecules of an adjacent granule. These double helices bind the two adjacent granules together and prevent amyloplast division. These fused granules have continuous outer layers, which consist of more amylose (Jiang et al., 2010) resulting from the increase in activity of granular-bound starch synthase at later stages of the kernel development (Sidebottom et al., 1998). The long-chain double helical crystallites formed from amylose molecules have melting temperatures above the boiling-water temperature, which retain the semi-crystalline structure and, in turn, maintain the granular shape of the elongated starch granules after thermally stable α-amylase hydrolysis at 95–100 °C (Jiang et al., 2010). In normal maize starch granules, amylose molecules are separated by amylopectin molecules (Jane et al., 1992; Kasemsuwan & Jane, 1994) because of the low concentration of amylose (Li et al., 2007). And the branch chains of amylopectin molecules are not long enough to form stable anti-parallel double helices between two adjacent granules in the normal maize amyloplast. Thus, two starch granules separate along with amyloplast division, and each remains with a newly-formed amyloplast (Fig. 4).

A proposed model of elongated starch granule formation is shown in Fig. 6. Two starch granules, each with hilum and growth rings, are initiated in an amyloplast (Fig. 6A). Then two granules begin fusing by forming anti-parallel amylose double helices between two growing granules, which prevent the amyloplast division (Fig. 6B). The two granules, after fusion, produce continuous outer layers (Fig. 6C). To the best of our knowledge, this mechanistic model is being proposed for the first time in this study, and assists the understanding of the formation of the elongated starch granules and RS formation in high-amylose maize starch.

Acknowledgements

The authors thank the USDA-ARS GEM project for the support of this research. The authors also wish to thank Randall Den Adel for assistance in preparing tissues for transmission electron microscopy in the Microscopy and NanoImaging Facility, and Margie Carter for assistance with confocal laser scanning microscopy.

References

AOAC. (2003). Association of Official Analytical Chemists (AOAC) official methods 991.43. Total, soluble, and insoluble dietary fiber in foods. In W. Horwithz (Ed.), *Official methods of analysis of the AOAC international*. Gaithersburg, Maryland: AOAC International.

Behall, K. M., & Howe, J. C. (1996). Resistant starch as energy. *Journal of the American College of Nutrition, 15*, 248–254.

Behall, K. M., Scholfield, D. J., & Hallfrisch, J. G. (2006a). Barley [beta]-glucan reduces plasma glucose and insulin responses compared with resistant starch in men. *Nutrition Research, 26*, 644–650.

Behall, K. M., Scholfield, D. J., Hallfrisch, J. G., & Liljeberg-Elmstaahl, H. G. M. (2006b). Consumption of both resistant starch and beta -glucan improves postprandial plasma glucose and insulin in women. *Diabetes Care, 29*, 976–981.

Boyer, C. D., Daniels, R. R., & Shannon, J. C. (1976). Abnormal starch granule formation in Zea-Mays-L endosperms possessing amylose-extender mutant. *Crop Science, 16*, 298–301.

Campbell, M. R., Jane, J., Pollak, L., Blanco, M., & O'Brien, A. (2007). Registration of maize germplasm line GEMS-0067. *Journal of Plant Registrations, 1*, 60–61.

Dronamraju, S. S., Coxhead, J. M., Kelly, S. B., Burn, J., & Mathers, J. C. (2009). Cell kinetics and gene expression changes in colorectal cancer patients given resistant starch: a randomised controlled trial. *Gut, 58*, 413–420.

Englyst, H. N., & Cummings, J. H. (1985). Digestion of the polysaccharides of some cereal food in the human small intestine. *American Journal of Clinical Nutrition, 42*, 778–787.

Englyst, H. N., & Macfarlane, G. T. (1986). Breakdown of resistant and readily digestible starch by human gut bacteria. *Journal of the Science of Food and Agriculture, 37*, 699–706.

French, D. (1984). Organization of starch granules. In R. L. Whistler, J. N. Bemiller, & E. F. Paschall (Eds.), *Starch: Chemistry and Technology* (pp. 183–247). New York: Academic Press.

Glaring, M. A., Koch, C. B., & Blennow, A. (2006). Genotype-specific spatial distribution of starch molecules in the starch granule: a combined CLSM and SEM approach. *Biomacromolecules, 7*, 2310–2320.

Higgins, J. A., Higbee, D. R., Donahoo, W. T., Brown, I. L., Bell, M. L., & Bessesen, D. H. (2004). Resistant starch consumption promotes lipid oxidation. *Nutrition & Metabolism, 1*, 8.

Horner, H. T., Healy, R. A., Ren, G., Fritz, D., Klyne, A., Seames, C., et al. (2007). Amyloplast to chromoplast conversion in developing ornamental tobacco floral nectaries provides sugar for nectar and antioxidants for protection. *American Journal of Botany, 94*, 12–24.

Jane, J., Xu, A., Radosavljevic, M., & Seib, P. A. (1992). Location of amylose in normal starch granules. I. Susceptibility of amylose and amylopectin to cross-linking reagents. *Cereal Chemistry, 69*, 405–409.

Jiang, H., Campbell, M., Blanco, M., & Jane, J. (2010) Characterization of maize amylose-extender (ae) mutant starches. Part II: Structures and properties of starch residues remaining after enzyme hydrolysis at boiling-water temperature. Carbohydrate Polymers, *80*, 1–12.

Kasemsuwan, T., & Jane, J. (1994). Location of amylose in normal starch granules. II. Locations of phosphodiester crosslinking revealed by phosphorus-31 nuclear magnetic resonance. *Cereal Chemistry, 71*, 282–287.

Li, L., Blanco, M., & Jane, J. (2007). Physicochemical properties of endosperm and pericarp starches during maize development. *Carbohydrate Polymers, 67*, 630–639.

Li, L., Jiang, H., Campbell, M., Blanco, M., & Jane, J. (2008). Characterization of maize amylose-extender (ae) mutant starches. Part I: Relationship between resistant starch contents and molecular structures. *Carbohydrate Polymers, 74*, 396–404.

Mercier, C., Charbonniere, R., Gallant, D., & Guilbot, A. (1970). Development of some characteristics of starches extracted from normal corn and amylomaize grains during their formation. *Staerke, 22*, 9–16.

Morell, M. K., Samuel, M. S., & O'Shea, M. G. (1998). Analysis of starch structure using fluorophore-assisted carbohydrate electrophoresis. *Electrophoresis, 19*, 2603–2611.

O'Shea, M. G., Samuel, M. S., Konik, C. M., & Morell, M. K. (1998). Fluorophore-assisted carbohydrate electrophoresis (FACE) of oligosaccharides: efficiency of labelling and high-resolution separation. *Carbohydrate Research, 307*, 1–12.

Pawlak, D. B., Kushner, J. A., & Ludwig, D. S. (2004). Effects of dietary glycaemic index on adiposity, glucose homoeostasis, and plasma lipids in animals. *Lancet, 364*, 778–785.

Perera, C., Lu, Z., Sell, J., & Jane, J. (2001). Comparison of physicochemical properties and structures of sugary-2 cornstarch with normal and waxy cultivars. *Cereal Chemistry, 78*, 249–256.

Richardson, P. H., Jeffcoat, R., & Shi, Y.-C. (2000). High-amylose starches: From biosynthesis to their use as food ingredients. *MRS Bulletin, 25*, 20–24.

Robertson, M. D., Bickerton, A. S., Dennis, A. L., Vidal, H., & Frayn, K. N. (2005). Insulin-sensitizing effects of dietary resistant starch and effects on skeletal muscle and adipose tissue metabolism. *American Journal of Clinical Nutrition, 82*, 559–567.

Robertson, M. D., Currie, J. M., Morgan, L. M., Jewell, D. P., & Frayn, K. N. (2003). Prior short-term consumption of resistant starch enhances postprandial insulin sensitivity in healthy subjects. *Diabetologia, 46*, 659–665.

Robyt, J. F. (1998). *Essentials of carbohydrate chemistry*. New York: Springer-Verlag.

Shannon, J. C., & Garwood, D. L. (1984). Genetics and physiology of starch development. In R. L. Whistler, J. N. Bemiller, & E. P. Paschall (Eds.), *Starch: chemistry and technology* (pp. 25–79). New York: Academic Press.

Shi, Y.-C., & Jeffcoat, R. (2001). Structural features of resistant starch. In B. McCleary & L. Prosky (Eds.), *Advanced dietary fibre technology* (pp. 430–439). Oxford, UK: Wiley-Blackwell.

Sidebottom, C., Kirkland, M., Strongitharm, B., & Jeffcoat, R. (1998). Characterization of the difference of starch branching enzyme activities in normal and low-amylopectin maize during kernel development. *Journal of Cereal Science, 27*, 279–287.

Van Munster, I. P., Tangerman, A., & Nagengast, F. M. (1994). Effect of resistant starch on colonic fermentation, bile acid metabolism, and mucosal proliferation. *Digestive Diseases and Sciences, 39*, 834–842.

Wolf, M. J., Seckinger, H. L., & Dimler, R. J. (1964). Microscopic characteristics of high-amylose corn starches. *Staerke, 16*, 377–382.

Wongsagonsup, R., Varavinit, S., & BeMiller, J. N. (2008). Increasing slowly digestible starch content of normal and waxy maize starches and properties of starch products. *Cereal Chemistry, 85*, 738–745.

Zhang, W., Wang, H., Zhang, Y., & Yang, Y. (2007). Effects of resistant starch on insulin resistance of type 2 mellitus patients. *Chinese Journal of Preventive Medicine, 41*, 101–104.